*Clays and Clay Minerals*, Vol. 35, No. 4, 241–250, 1987.

# HYDROTHERMAL TREATMENT OF SMECTITE, ILLITE, AND BASALT TO 460°C: COMPARISON OF NATURAL WITH HYDROTHERMALLY FORMED CLAY MINERALS

YU-CHYI YAU, DONALD R. PEACOR, ERIC J. ESSENE,
JUNG H. LEE,[2] LUNG-CHUAN KUO,[3] AND MICHAEL A. COSCA

Department of Geological Sciences, The University of Michigan
Ann Arbor, Michigan 48109

**Abstract**—Wyoming bentonite, Fithian illite, and basalt from the Umtanum Formation, Washington, were treated hydrothermally at 200° to 460°C and 260 to 500 bars for 71 to 584 days. No change was detected for the bentonite and basalt, except for the loss of calcite and exchange of Ca for K in the smectite and the growth of a small amount of smectite (presumably from a glass phase) in the basalt. Calcite in the initial bentonite may have stabilized the smectite by Ca/K exchange; thus, if the latter is used as a packing material in a nuclear waste repository, limestone should be added. No change was detected in the illite samples treated <300°C; however, at 360°C, euhedral crystals of berthierine and illite grew at the expense of original illite/smectite, apparently by a solution-crystallization process. Significant changes involving the dissolution of starting phases and the formation of illite and chlorite were also detected in mixtures of basalt and bentonite at 400°C; at temperatures <400°C, no changes were observed.

The newly formed mineral phases (berthierine, illite, and chlorite) observed by transmission electron microscopy showed euhedral to subhedral shapes. These shapes are the same as those observed in hydrothermally altered sediments from the Salton Sea field and different from those from burial metamorphic environments, such as Gulf Coast sediments. The reaction mechanism is apparently the dissolution of reactants followed by the crystallization of products from solution, without conservation of structural elements of the reactants. Reactions apparently required temperatures greater than those for analogous changes in nature, suggesting that the degree of reaction was controlled by kinetics. The lack of dissolution in experimental runs at low temperatures, however, does not necessarily imply long-term stabilities of these clay minerals.

**Key Words**—Basalt, Berthierine, Hydrothermal, Illite, Smectite, Stability.

## INTRODUCTION

Storage of high-level nuclear waste in subsurface repositories usually involves a clay-bearing packing material that acts as a physicochemical barrier between solid waste canisters and the host rock (Komarneni and Roy, 1980). Packing materials may react with ground water at temperatures of as much as 300°C and pressures of several hundred bars. Chemical, structural, and textural changes due to such reactions may degrade the packing performance over the projected life of the repository (e.g., 10,000 years). To evaluate the potential for such changes many workers have carried out hydrothermal experiments on candidate packing materials under conditions thought to be analogous to those of the proposed repositories (see, e.g., McCarthy *et al.*, 1978; Komarneni and Roy, 1980; Inoue, 1983; Howard and Roy, 1985).

We have studied the hydrothermal stability of three candidate packing materials—bentonite, illite, and basalt—at temperatures, pressures, and chemical conditions similar to those expected in a nuclear-waste repository (Apted and Myers, 1982; Fergusson, 1982; Savage and Chapman, 1982). These conditions are analogous to those prevailing during sediment diagenesis. In particular, they are similar to those prevailing during hydrothermal metamorphism of sediments in geothermally active regions, such as the Salton Sea, which serves as a natural analogue of a repository system (Elders and Moody, 1985). From a comparison of the textures, structures, and chemistry of the products of our hydrothermal experiments and those of equivalent phases from natural systems we show here that the experimental products are analogous to those in the Salton Sea region and very different from those in other sedimentary systems.

## EXPERIMENTAL

### *Measurements*

Starting materials and products were characterized by X-ray powder diffraction (XRD), scanning electron microscopy coupled with energy dispersive analyses (SEM/EDX), and transmission (TEM) and analytical electron microscopy (AEM) (Blake *et al.*, 1980; Lee *et al.*, 1984; Yau *et al.*, 1987). Weight percentages of each mineral were estimated by XRD using integrated in-

[1] Contribution No. 430 from the Mineralogical Laboratory, Department of Geological Sciences, The University of Michigan, Ann Arbor, Michigan 48109.

[2] Present address: Department of Geology, Jeonbuk National University, Jeonju, Republic of Korea.

[3] Present address: 6467 R&D West, Conoco, Ponca City, Oklahoma 74601.

tensities and standard curves for each phase relative to quartz as an internal standard.

*Starting materials*

*Wyoming bentonite.* The Wyoming bentonite (commercial brand, Envirogel 200) consists of about 85% smectite, 7% calcite, 7% quartz, and 1% illite. The smectite gives a sharp 001 peak at a d value of 12.5 Å which expands to 16.6 Å with ethylene glycol treatment. SEM revealed that the smectite typically occurs as stacked platelets (Figure 1a). Quartz and calcite occur as granular aggregates or discrete grains. The SEM/EDX spectra obtained from the smectite verifies that Na is the most abundant interlayer cation, with subordinate K and Ca (Figure 1b). Measurable quantities of Fe and Mg are also present, apparently substituting for Al in octahedral sites.

The typical texture of smectite observed by TEM consists of an irregular stacking of layers having no well-defined crystal outlines (Figure 2a). Electron diffraction patterns of the unglycolated sample (insert in Figure 2a) show that most of the smectite layers have a basal spacing of 13.0 Å, consistent with a hydrated smectite. Higher magnification lattice-fringe images of smectite reveal discontinuous, curved layers associated with abundant individual layer terminations (Figure 2b); such imperfections are common in smectites (Page, 1980; Lee *et al.*, 1985; Ahn and Peacor, 1986). The fringes show wide variations in spacings between different layers and along an individual layer. Some layers have spacings as small as 10 Å, presumably due to collapse of an original 13-Å layer upon loss of water in the TEM vacuum.

*Fithian illite.* Illite from the type locality, Fithian, Illinois was shown by XRD to contain about 30% of an expandable component in the clay fraction. Quartz and feldspars make up about 45% of the sample. Illite occurs as packets of layers separated by smectite layers (Figure 2c), similar to illite in Gulf Coast shales (Ahn and Peacor, 1986). The illite layers are characterized by mottled contrast, presumably due to strain associated with beam damage induced by diffusion of K or Na (Ahn *et al.*, 1986). Layers within a packet are relatively straight and continuous, although low-angle grain boundaries characterized by concentrated layer terminations are abundant between illite packets. AEM analyses show that the illite is chemically heterogeneous, especially in the octahedral components Mg, Fe, and Al (Figure 4a). The dominant interlayer cation is K, with subordinate Na and Ca.

*Umtanum basalt.* Basalt from the Umtanum Formation, well DC-6, Hanford, Washington, is dark gray, homogeneous, and fine grained. In thin section, it displays hyalopilitic texture characterized by the presence of as much as 30% silicate glass interstitial to plagioclase laths and euhedral to subhedral augites. Magnetite microphenocrysts are ubiquitous. SEM studies reveal abundant cracks in the basalt along which a variety of secondary minerals have been deposited, including opaline materials, zeolites, and iron oxides. The basalt used in the hydrothermal experiments was carefully selected to avoid such materials. Two apparently immiscible glasses were noted by TEM (Figure 2d); AEM analysis demonstrated that one of the glasses is rich in K (see Kuo *et al.*, 1986).

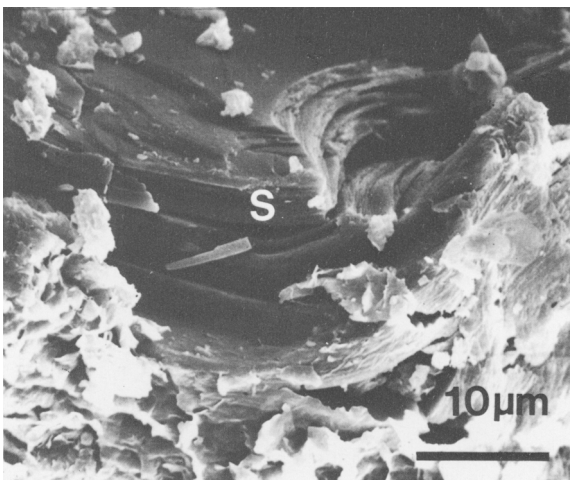


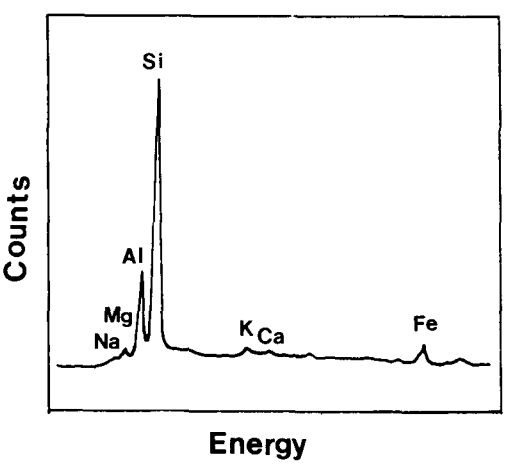


Figure 1. (upper) Scanning electron microscopic image of smectite (S) in untreated bentonite, showing layered appearance. (lower) Energy dispersive X-ray spectrum of the smectite shown above.

*Hydrothermal experiments*

Hydrothermal experiments were carried out in TemPres cold-seal pressure vessels. The temperatures were regulated with Eurotherm solid-state, proportional temperature controllers. Powdered samples (0.03–0.07 g) were placed in welded gold or silver tubing, containing 0.02–0.1 $cm^3$ of solution. There is effectively no diffusion of $H_2$ through such capsules during the experiments (Chou, 1986). Redox equilibria are buffered during the experiments by the rock chemistry. The

https://doi.org/10.1346/CCMN.1987.0350401 Published online by Cambridge University Press

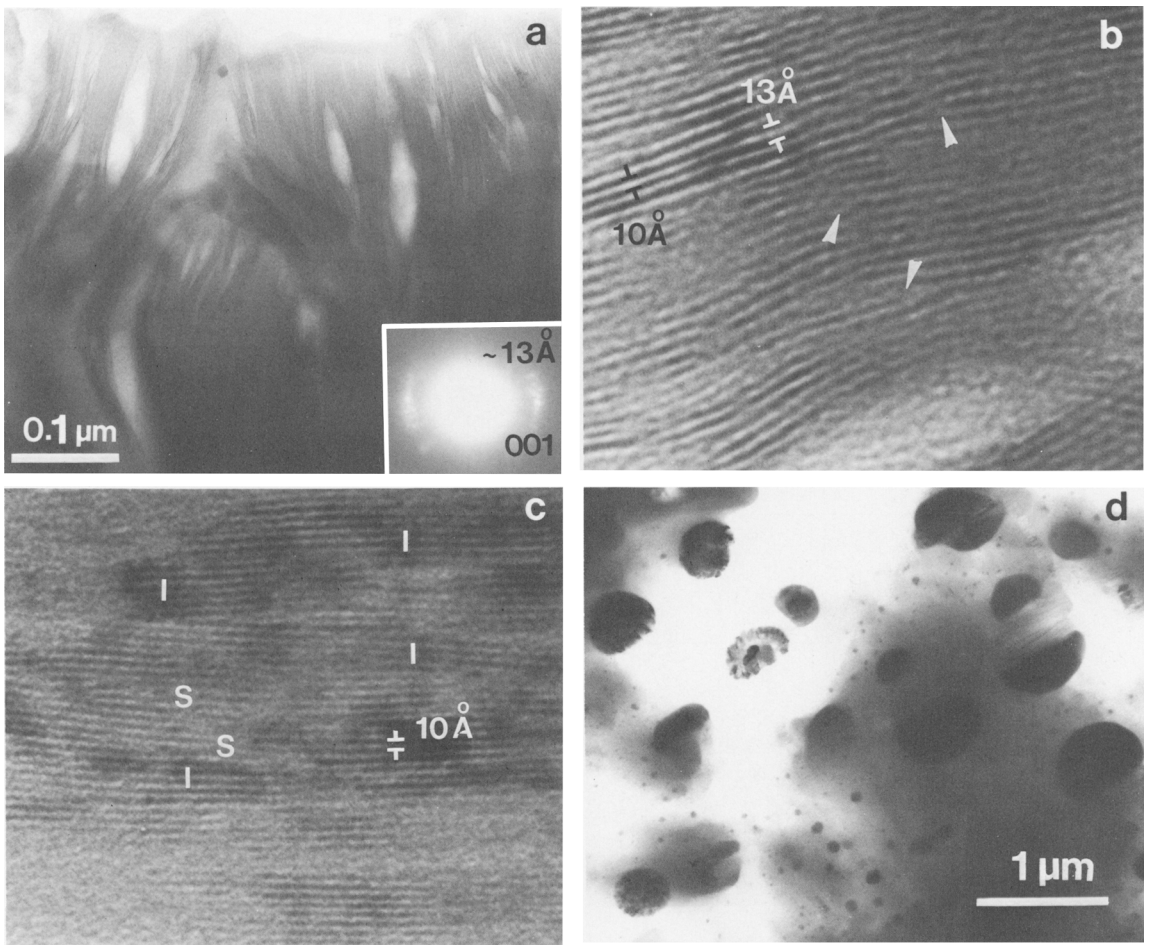


Figure 2. Transmission electron microscopic images of untreated smectite, illite, and basalt. (a) Low magnification image of smectite and its corresponding electron diffraction pattern showing d(001) = 13 Å on average. (b) Lattice-fringe images of smectite showing typical variations in layer spacings and abundant layer terminations (arrows). (c) Lattice-fringe images of Fithian illite exhibiting packets of 10-Å illite layers (I) separated by smectite layers (S). (d) Immiscible glass in the Umtanum basalt shows randomly distributed, dark glass globules in light colored glass matrix.

fluid/rock ratio of each charge was estimated from the weight ratio. Temperature and pressure were monitored by chromel-alumel thermocouples using a potentiometer and pressure gauges calibrated by the manufacturer. Variations in temperatures and pressures never exceeded 2%. Charges were weighed before and after experiments to verify that the capsules remained sealed for the duration of the experiments.

The general experimental conditions were: (1) The temperature ranged from 100° to 300°C, representing the maximum and long-term temperatures expected in a waste repository (Apted and Myers, 1982); temperatures as high as 460°C were also used to accelerate reaction rates. (2) The fluid/rock ratios ranged from 0.3 to 10, typical of natural hydrothermal fields (e.g., Savage and Chapman, 1982). (3) The duration of experiments was from 71 to 584 days. (4) The pressure ranged from 300 to 500 bars. (5) The solution chem-

Table 1. Chemical composition (ppm) of ground water in the Umtanum Formation, Pasco Basin, Washington, compared with sea water and river water compositions.

| Species | 1 | 2 | 3 | 4 |
|---|---|---|---|---|
| $Na^+$ | 10,540 | 6.3 | 270 | 270 |
| $K^+$ | 380 | 2.3 | 6 | 6 |
| $Ca^{2+}$ | 400 | 15.0 | 2 | 2 |
| $Mg^{2+}$ | 1270 | 4.1 | 0.3 | — |
| $H_4SiO_4$ | — | 34.9 | 120 | — |
| $Cl^-$ | 18,980 | 7.8 | 190 | 190 |
| $F^-$ | 1.3 | — | 32 | 32 |
| $SO_4^{2-}$ | 2450 | 11.2 | 120 | 120 |
| $HCO_3^-$ | 140 | 58.4 | 60 | 101 |
| $CO_3^{2-}$ | — | — | — | 22 |

1. Average sea water (from Fergusson, 1982).
2. Average river water (from Fergusson, 1982).
3. Ground water, Umtanum Formation.
4. Simulated ground water used in the present experiment (pH buffered to 9.5 using carbonate/bicarbonate ions).

https://doi.org/10.1346/CCMN.1987.0350401 Published online by Cambridge University Press

Table 2. Experimental run conditions and results.

| Charge | T (°C) | P (bar) | Time (day) | Fluid/rock (wt. ratio) | Results |
|---|---|---|---|---|---|
| Bentonite | 200 | 300 | 537 | 1.75 | |
| | 300 | 300 | 91 | 0.44 | Calcite lost, Ca-K exchange |
| | 300 | 500 | 71 | 0.50 | occurred in smectite |
| | 300 | 500 | 537 | 5.00 | |
| Illite | 200 | 300 | 552 | 1.23 | No change |
| | 300 | 350 | 91 | 0.40 | No change |
| | 300 | 300 | 584 | 1.05 | Growth of berthierine and |
| | 350 | 300 | 91 | 0.58 | illite |
| | 360 | 300 | 97 | 0.42 | No change |
| | 460 | 300 | 92 | 0.52 | No change |
| Basalt | 200 | 300 | 552 | 1.75 | No change |
| | 300 | 350 | 91 | 0.34 | No change |
| | 300 | 300 | 584 | 1.09 | No change |
| | 360 | 300 | 97 | 1.85 | Growth of smectite |
| 75% basalt | 300 | 300 | 152 | 0.09 | No change |
| 25% bentonite | 400 | 300 | 81 | 2.08 | Growth of wairakite |
| 25% basalt | 300 | 300 | 334 | 1.85 | No change |
| 75% bentonite | 400 | 300 | 280 | 1.03 | Wairakite + chlorite |
| 50% basalt | 300 | 300 | 334 | 1.15 | No change |
| 50% bentonite | 400 | 300 | 280 | 1.22 | Chlorite + illite |

istry of an artificial solution had cation concentrations and pH equal to those of the repository ground water (Table 1; Fergusson, 1982).

## RESULTS

Experimental conditions and results are summarized in Table 2 and described in detail below:

### *Bentonite*

No significant changes were detected in the bentonite samples after hydrothermal treatments except for the loss of calcite. Examination by TEM showed that the lattice-fringe images of smectite in the treated material were identical to those observed in the starting material; however, AEM analyses of the treated bentonite revealed an increase in Ca and decrease in K, with no detectable changes in other elements. These data suggest that Ca exchanged for K in the smectite interlayer due to calcite dissolution.

### *Fithian illite*

No changes were detected by XRD in samples treated at 300°C for 71 to 91 days or in those treated at 200°C for 414 to 552 days. XRD patterns of products of 300°C runs of longer duration (432 to 584 days), as well as those from higher temperature runs, however, showed a new 7-Å peak. Furthermore, the 001 peak of illite was significantly less diffuse and asymmetric than that of the starting material, indicating that at least some of the illite had recrystallized.

Low-magnification TEM (Figure 3a) of products showed individual euhedral crystals, each a few hundred angstrom units in thickness. The discrete, well-defined crystals are in sharp contrast with the texture of the starting material, in which no subhedral to euhedral phyllosilicate crystals were noted (cf. Figure 2c). Electron diffraction patterns from these crystals displayed both 10- and 7-Å 001 reflections (Figure 3b), consistent with the XRD data. At high magnification, euhedral crystals consisting only of 10-Å or 7-Å layers were observed (Figure 3c). In addition, 10- and 7-Å layers were also noted as packets of layers intergrown within a single crystal (Figure 3d). These textures clearly demonstrate that both phases formed during the same event through solution-crystallization.

The EDX spectra obtained from the 10-Å phase confirm that it is illite with minor Mg and Fe (Figure 4b). Comparison of the EDX spectrum of the starting illite (Figure 4a) with the newly formed illite shows that the latter is richer in K and Al relative to Si, suggesting reaction of illite towards muscovite (Hower *et al.*, 1976; Ahn and Peacor, 1986). After subtraction of illite components, an EDX spectrum (Figure 4c) of a mixture of the 7-Å phase and illite implies that the 7-Å phase is rich in Fe and Mg, with minor Al presumably in the octahedral sites. The 7-Å phase therefore appears to be berthierine, an iron, aluminum-rich 1:1 phyllosilicate (Bailey, 1980; Brindley, 1982), which may form as a metastable precursor of chlorite at low temperature (Yoder, 1952; Nelson and Roy, 1958; Ahn and Peacor, 1985a).

### *Basalt*

No differences were detected between the treated and untreated basalt for both the 200° and 300°C runs. For the 360°C runs, however, a new weak reflection at 14

https://doi.org/10.1346/CCMN.1987.0350401 Published online by Cambridge University Press

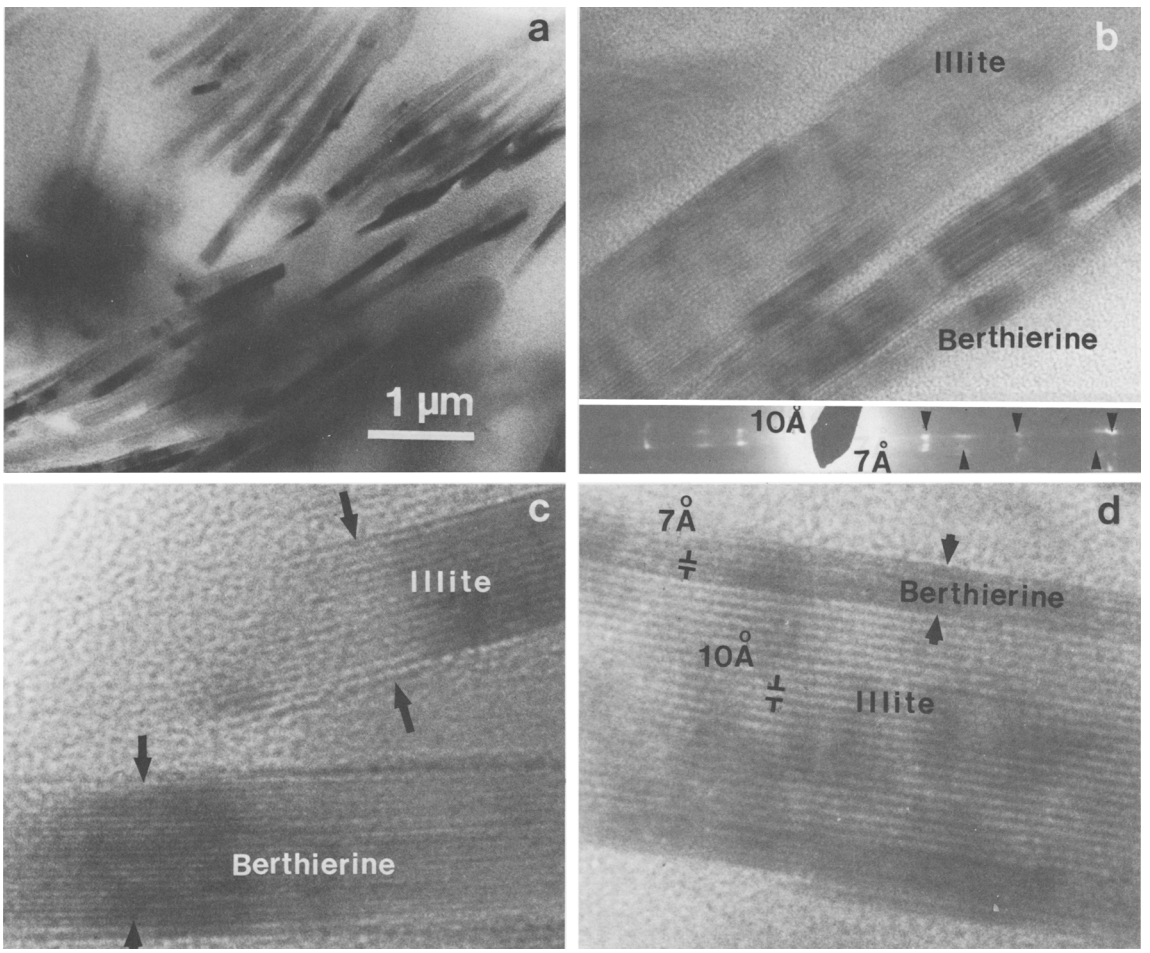


Figure 3. Transmission electron microscopic images of run-products from Fithian illite. (a) Low-magnification image showing discrete, euhedral to subhedral crystals. (b) Crystals of illite and berthierine identified by their lattice fringes and corresponding electron diffraction pattern. (c) High-magnification image showing separate grains of illite and berthierine. (d) Layers of illite and berthierine intergrown as part of a single grain.

Å was found in the XRD patterns, indicating the formation of smectite, chlorite, or vermiculite. Feathery clay flakes were noted also by SEM. Qualitative EDX analyses obtained using the SEM indicated that compositionally the clay is a smectite or an interlayered illite/smectite. Unfortunately, the smectite produced was not characterized by TEM/AEM.

*Basalt + bentonite*

XRD patterns of basalt-bentonite mixtures treated at 300°C were almost unchanged compared with those of the starting materials. The only difference was the presence in all patterns of a weak peak corresponding to the strongest peak of wairakite. SEM images showed crystals displaying morphology typical of wairakite. The wairakite identification was supported by EDX spectra, which showed major peaks of Ca, Al, and Si. Smectite remained abundant in the run products. Because the starting crystalline materials appear to have been largely unchanged by hydrothermal treatment, the wairakite may have formed from the glass in the basalt.

XRD patterns for 400°C run-products of each of the basalt-bentonite mixtures are shown in Figure 5. Pattern B (75% basalt) is very similar to that of the starting material, except for the presence of some peaks of wairakite, as noted above for the 300°C run-products. Patterns A (50% basalt) and C (25% basalt), however, show considerable change. Pattern C shows the presence of substantial chlorite and wairakite and the absence or near absence of smectite and pyroxene (and, presumably, glass). Pattern A (50% basalt) shows no peaks of the starting minerals, only those of chlorite and illite.

TEM of the run-products of 50% bentonite + 50% basalt show euhedral to subhedral phyllosilicate particles having thicknesses of from 300 Å to a few micrometers (Figure 6a). The euhedral character is similar

https://doi.org/10.1346/CCMN.1987.0350401 Published online by Cambridge University Press

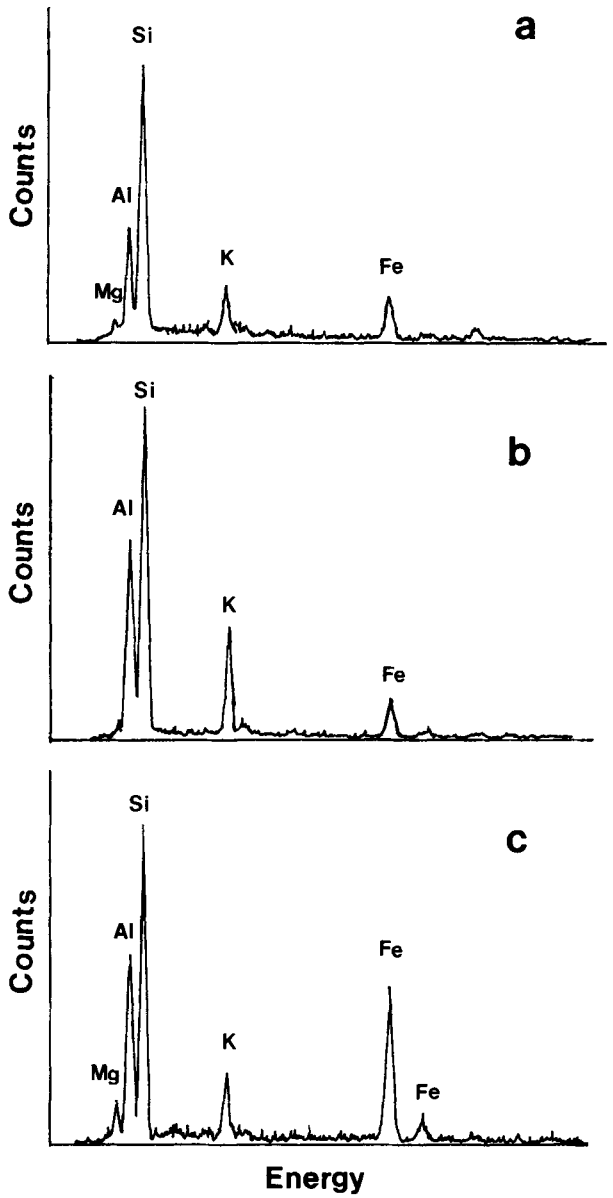


Figure 4. Energy dispersive X-ray spectra obtained by analytical electron microscopy from (a) Fithian illite starting material, (b) discrete illite crystal in run-product, (c) unresolved berthierine and illite.

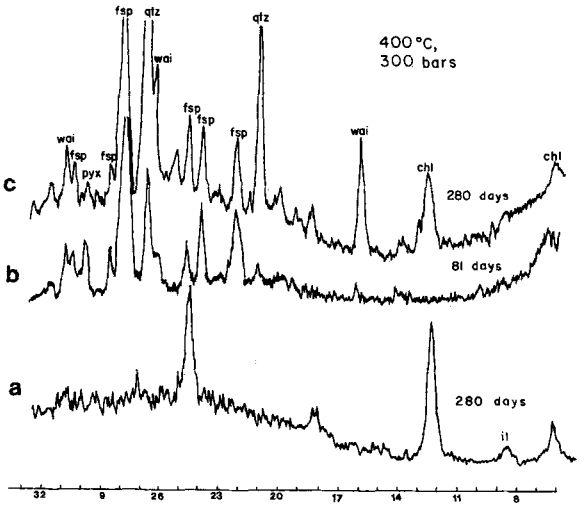


Figure 5. X-ray diffraction patterns of products of runs using basalt-bentonite mixtures. (a) Product of 50% basalt + 50% bentonite showing only chlorite and illite. (b) Product of 75% basalt + 25% bentonite showing almost all of the starting phases. (c) Product of 25% basalt + 75% bentonite; chlorite and wairakite are major new phases (wai = wairakite, fsp = feldspar, pyx = pyroxene, qtz = quartz, chl = chlorite, and il = illite). Abscissa axis is in terms of °2$\theta$, CuK$\alpha$ radiation.

to that shown in Figure 3a, although 14-Å chlorite is present in the former product instead of 7-Å berthierine found here. From high-magnification micrographs, these crystals consist of 10-Å layers, 14-Å layers, or a mixture of 10- and 14-Å layers. The 14-Å chlorite is more common than the 10-Å illite, consistent with XRD data. The layers within each crystal are commonly free of imperfections (Figure 6b). Where mixed 10- and 14-Å layers are present, the number of identical, adjacent layers varies from 1 to 10, resulting in complex mixed-layered sequences (Figure 6c). Short-range ordered, 1:1 mixed layering of illite and chlorite can be seen locally in Figure 6d having regular repeats of 24 Å.

EDX spectra from the crystals having 10-Å layers are similar to that shown in Figure 4b, suggesting that the 10-Å phase is illite. The spectra obtained from the 14-Å crystals (Figure 7) include major peaks of Si, Mg, Fe, and Al, consistent with trioctahedral chlorite.

## DISCUSSION

### *Experimental synthesis compared to natural formation*

Smectite is probably metastable with respect to illite (±chlorite), and illite is probably metastable with respect to muscovite (±pyrophyllite) at high temperature and pressure (Velde and Hower, 1963; Maxwell and Hower, 1967; Burst, 1959; Frey, 1970; Kossovskaya and Drits, 1970; Perry and Hower, 1970; Hower *et al.*, 1976). Many field studies have shown that smectite reacts to form illite at temperatures <200°C and that illite reacts to form muscovite at temperatures approaching 300°C; however, smectite persisted during these experimental time periods to temperatures as high as 360°C. The samples of disordered illite and associated smectite were also largely unchanged in experiments at 200°C and in some runs at 300°C.

Ahn and Peacor (1986) studied the microstructural changes for the smectite-to-illite reaction and suggested that the rate of transition is determined by reconstruction of and chemical changes in the basic tetrahedral and octahedral layers. Lee *et al.* (1986) inferred that

https://doi.org/10.1346/CCMN.1987.0350401 Published online by Cambridge University Press

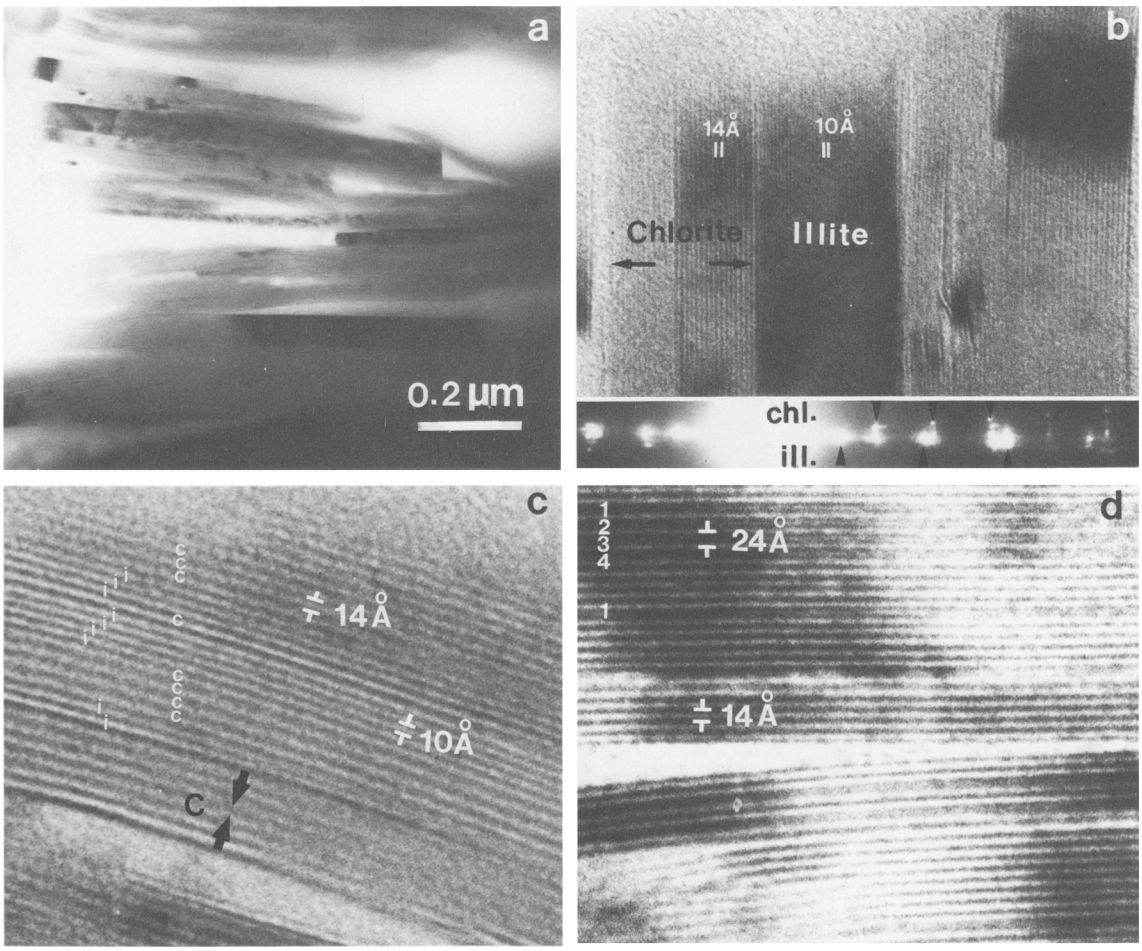


Figure 6. Transmission electron microscopic images of run-products of 50% basalt + 50% bentonite. (a) Low-magnification image showing discrete, subhedral crystals. (b) Separate packets of illite and chlorite are identified by their fringes and corresponding electron diffraction pattern. (c) Complex mixed-layering of illite (i) and chlorite (c). (d) Short-range ordered 1:1 illite/chlorite mixed-layering resulting in four repeats of 24 Å.

the transition of illite toward muscovite involves tetrahedral bond rupturing and reconstitution. Such transformations are very sluggish, and the lack of observed reaction is therefore to be expected at low temperatures. Thus, smectite, illite, and basalt may persist metastably in a repository environment, but the lack of change over the relatively short time periods of the experiments does not imply that these materials are thermodynamically stable.

*Formation of berthierine, chlorite, and illite/chlorite*

In the present study, 7-Å berthierine layers formed as a product of reaction of the Fithian illite treated at 300°C for 584 days and at 350°–460°C for 90 days. A 14-Å chlorite, however, was identified in mixtures containing 50% or more bentonite with basalt treated at 400°C for 280 days. Qualitative chemical data imply that the berthierine and chlorite are similar in composition. Because the illite/smectite is the only phase containing Mg and Fe in the Fithian illite sample, the Mg and Fe necessary for the formation of berthierine must have been derived from the illite/smectite. Many studies have also suggested that berthierine and chlorite form as by-products of smectite-to-illite reactions utilizing the Mg and Fe released from smectite during diagenesis (e.g., Hower *et al.*, 1976; Ahn and Peacor, 1985a).

In studies of chlorite synthesis, many investigators have observed that a 7-Å phase precedes the formation of chlorite; they have suggested that the 7-Å phase either is a stable low-temperature polymorph of the 14-Å chlorite or forms metastably with respect to chlorite (Yoder, 1952; Nelson and Roy, 1958; Gillery, 1959; Velde, 1973). Natural 7-Å berthierine has been found intercalated with chlorite in shallow sediments undergoing diagenesis, but it has not been found in deep sediments (Ahn and Peacor, 1985a). Ahn and

https://doi.org/10.1346/CCMN.1987.0350401 Published online by Cambridge University Press

Peacor pointed out that the 7-Å phase is apparently metastable relative to the 14-Å chlorite in that it usually forms by rapid crystallization at low temperatures where kinetic effects are favorable. Studies of clinochlore (Cho and Fawcett, 1986) show that the conversion of 7-Å chlorite to 14-Å chlorite requires a large activation energy (90 ± 35 kcal/mole, at <670°C), indicating that the conversion involves rearrangements of Si–O bonds. The formation of berthierine in the short-term and lower temperature runs of this study is also compatible with berthierine being metastable relative to chlorite.

Random and short-range 1:1 ordered illite/chlorite mixed-layering were common in the products of smectite-basalt mixtures. Because both illite and chlorite were newly formed minerals in the experimental products, the illite/chlorite is inferred to have formed by primary growth rather than by replacement. Dioctahedral illite and trioctahedral chlorite mixed-layer phases have also been observed in natural samples (Page and Wenk, 1979; Knipe, 1979; Lee *et al.*, 1984; Ahn and Peacor, 1985b). In addition, 1:1 ordered chlorite/illite (Lee and Peacor, 1985) was also described by Lee and Peacor (1985) who pointed out that the ordered 1:1 illite/chlorite units should be found only as metastable structures at low temperature. The mixed-layered phase observed in the present experiments is consistent with such a relation in that it formed rapidly under experimental conditions.

*Formation mechanisms of illite from smectite*

Although almost no changes in the clays were noted at low temperatures, two major changes were observed in experiments carried out at higher temperatures (>300°C): (1) dissolution of illite/smectite and the production of euhedral illite and berthierine; and (2) dissolution of starting phases in mixtures of basalt + bentonite and crystallization of illite and chlorite. All the new mineral phases formed euhedral to subhedral crystals having textures similar to those observed by Yau *et al.* (1987) in hydrothermally altered sediments from the Salton Sea geothermal field, where detrital illite/smectite has completely dissolved with subsequent crystallization of illite and chlorite as discrete euhedral grains. These textures are distinct from those observed in a typical pelitic burial sequence, such as that described by Ahn and Peacor (1986) in Gulf Coast sediments.

By contrasting the textural and structural relations in the Gulf Coast and the Salton Sea shales, Ahn and Peacor (1986) and Yau *et al.* (1987) described two different formation mechanisms for illite as a product of smectite. The mechanism proposed for the Gulf Coast material involves formation of embryonic thin packets of illite layers within smectite, which increase in size by gradually consuming surrounding smectite layers. This mechanism is simple replacement, although it requires solution and crystallization that is localized across a replacement reaction front. The resulting illite forms an irregular, continuous, anhedral matrix to detrital phases, as does the original smectite, and there is no suggestion of regular crystal form. In contrast, the Salton Sea model involves complete dissolution of smectite, transportation of components through a pore fluid, and precipitation of illite at a site separate from original smectite; euhedral to subhedral, platy illite also forms in open pore space. Yau *et al.* (1987) attributed the different mechanisms to differences in the porosity and permeability of the sediments. The similarity in texture of samples from the present study to that observed in the Salton Sea system is not unexpected because both systems are characterized by relatively high porosity. Smectite in these two systems is in direct contact with pore fluids which facilitate dissolution of reactants, transport of ions, and precipitation of products. Thus, the Salton Sea geothermal system may be regarded as a natural analogue of a repository system (Elders and Moody, 1985). Moreover, hydrothermal metamorphism in the Salton Sea system may be only 16,000 years old (Kistler and Obradovich, in Muffler and White, 1969), an age similar to the proposed life of a repository (10,000 years). Thus, reactions that have occurred in the Salton Sea system may also take place in the repository environment in the presence of pore fluids at similar temperatures; however, control of porosity/permeability relations may retard reactions and allow retention of metastable phases. The similarity in hydrothermal experiments and Salton Sea clays and the dissimilarity with Gulf Coast clays imply that caution should be used in applications of results of hydrothermal experiments to Gulf Coast-like systems, where the reaction mechanisms and textures are different.

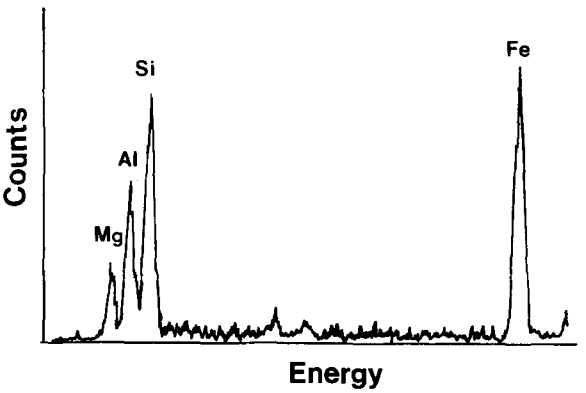


Figure 7. Energy dispersive X-ray spectrum for chlorite formed as a hydrothermal run-product (50% basalt + 50% bentonite starting material).

## ACKNOWLEDGMENTS

We thank Susan Penoyar for her help in sample characterization and W. C. Bigelow and the staff of the

University of Michigan Electron Microbeam Analysis Laboratory for their efforts in maintaining the SEM and STEM instruments. This study was supported by the U.S. Nuclear Regulatory Commission under contract No. 31-109-Eng-38 through the Argonne National Laboratory to D. R. Peacor and E. J. Essene and by National Science Foundation (NSF) grants EAR-83-13236 and EAR-86-04170 to D. R. Peacor. The STEM used in this study was acquired under Grant No. DMR-77-09643 from the NSF.

## REFERENCES

Ahn, J. H. and Peacor, D. R. (1985a) Transmission electron microscopic study of diagenetic chlorite in Gulf Coast argillaceous sediments: *Clays & Clay Minerals* **33,** 228–237.

Ahn, J. H. and Peacor, D. R. (1985b) TEM study of mineralogy and diagenesis of phyllosilicates in volcanogenic sediments from the Southland Syncline, New Zealand: *Geol. Soc. America, Abstr. Prog.* **17,** p. 510.

Ahn, J. H. and Peacor, D. R. (1986) Transmission and analytical electron microscopy of the smectite-to-illite transition: *Clays & Clay Minerals* **34,** 165–179.

Ahn, J. H., Peacor, D. R., and Essene, E. J. (1986) Cation-diffusion induced characteristic beam damage in transmission electron microscope images of micas: *Ultramicroscopy* **19,** 375–382.

Apted, M. J. and Myers, J. (1982) Comparison of the hydrothermal stability of simulated spent fuel and borosilicate glass in a basaltic environment. *Rockwell Hanford Operations Rept.* **RHO-RW-ST-38 P,** 101 pp.

Bailey, S. W. (1980) Structures of layer silicates: in *Crystal Structures of Clay Minerals and their X-ray Identification,* G. W. Brindley and G. Brown, eds., Mineralogical Society, London, 1–123.

Blake, D. F., Allard, L. F., Peacor, D. R., and Bigelow, W. C. (1980) Biomineralization in crinoid echinoderms: Characterization of crinoid skeletal elements using TEM and STEM microanalysis: *Scanning Electron Microscopy/1981,* **3,** 321–328.

Brindley, G. W. (1982) Chemical compositions of berthierines—A review: *Clays & Clay Minerals* **30,** 153–155.

Burst, J. F., Jr. (1959) Post-diagenetic clay mineral environmental relationships in the Gulf Coast Eocene: in *Clays and Clay Minerals, Proc. 6th Natl. Conf., Berkeley, California, 1957,* Ada Swineford, ed., Pergamon Press, New York, 327–341.

Cho, M. and Fawcett, J. J. (1986) A kinetic study of clinochlore and its high temperature equivalent forsterite-cordierite-spinel at 2 kbar water pressure: *Amer. Mineral.* **71,** 68–78.

Chou, I-M. (1986) Permeability of precious metals to hydrogen at 2kb total pressure and elevated temperatures: *Amer. J. Sci.* **286,** 638–658.

Elders, W. A. and Moody, J. B. (1985) The Salton Sea geothermal field as a natural analog for the near-field in a salt high-level nuclear waste repository: *The Scientific Basis for Nuclear Waste Management, Proc. Materials Research Society Symp., Vol. 44,* C. M. Jantzen, J. A. Stone, and R. C. Ewing, eds., 565–572.

Fergusson, J. E. (1982) *Inorganic Chemistry and the Earth:* Pergamon Press, New York, 440 pp.

Frey, M. (1970) The step from diagenesis to metamorphism in pelitic rocks during Alpine orogenesis: *Sedimentology* **15,** 261–279.

Gillery, F. H. (1959) The X-ray study of synthetic Mg-Al serpentines and chlorites. *Amer. Mineral.* **44,** 143–149.

Howard, J. J. and Roy, D. M. (1985) Development of layer charge and kinetics of experimental smectite alteration: *Clays & Clay Minerals* **33,** 81–88.

Hower, J., Eslinger, E. V., Hower, M. E., and Perry, E. A. (1976) Mechanism of burial metamorphism of argillaceous sediment: 1. Mineralogical and chemical evidence: *Geol. Soc. Amer. Bull.* **87,** 725–737.

Inoue, A. (1983) Potassium fixation by clay minerals during hydrothermal treatment: *Clays & Clay Minerals* **27,** 393–401.

Knipe, R. J. (1979) Chemical changes during slaty cleavage development: *Bull. Miner.* **102,** 206–209.

Komarneni, S. and Roy, R. (1980) Hydrothermal transformations in candidate overpack materials and their effects on cesium and strontium sorption: *Nucl. Tech.* **54,** 118–122.

Kossovskaya, A. G. and Drits, V. A. (1970) The variability of micaceous minerals in sedimentary rocks: *Sedimentology* **15,** 83–101.

Kuo, L. C., Lee, J. H., Essene, E. J., and Peacor, D. R. (1986) Occurrence, chemistry and origin of immiscible silicate glasses in a tholeiitic basalt: A TEM/AEM study. *Contrib. Miner. Petrol.* **94,** 90–98.

Lee, J. H. and Peacor, D. R. (1985) Ordered 1:1 interstratification of illite and chlorite: A transmission and analytical electron microscopy study: *Clays & Clay Minerals* **33,** 463–467.

Lee, J. H., Ahn, J., and Peacor, D. R. (1985) Textures in layered silicates: Progressive changes through diagenesis and low-temperature metamorphism: *J. Sed. Petrol.* **55,** 532–540.

Lee, J. H., Peacor, D. R., Lewis, D. D., and Wintsch, R. P. (1984) Chlorite-illite/muscovite interlayered and interstratified crystals: A TEM-AEM study: *Contrib. Mineral. Petrol.* **88,** 372–385.

Lee, J. H., Peacor, D. R., Lewis, D. D., and Wintsch, R. P. (1986) Evidence for syntectonic crystallization for the mudstone to slate transition at Lehigh Gap, Pennsylvania: *J. Struct. Geol.* **8,** 767–780.

Maxwell, D. and Hower, J. (1967) High-grade diagenesis and low-grade metamorphism of illite in the Precambrian Belt Series: *Amer. Mineral.* **52,** 843–857.

McCarthy, G. J., White, W. B., Roy, R., Scheetz, B. E., Komarneni, S., Smith, D. K., and Roy, D. M. (1978) Interactions between nuclear waste and surrounding rock: *Nature* **273,** 216–217.

Muffler, L. J. P. and White, D. E. (1969) Active metamorphism of Upper Cenozoic sediments in the Salton Sea Geothermal field and the Salton Trough, southeastern California. *Geol. Soc. Amer. Bull.* **80,** 157–182.

Nelson, B. W. and Roy, R. (1958) Synthesis of the chlorites and their structural and chemical constitution: *Amer. Mineral.* **43,** 707–725.

Page, R. H. (1980) Partial interlayers in phyllosilicates studied by transmission electron microscopy: *Contrib. Miner. Petrol.* **75,** 309–314.

Page, R. and Wenk, H. R. (1979) Phyllosilicate alteration of plagioclase studied by transmission electron microscopy: *Geology* **7,** 393–397.

Perry, E. and Hower, J. (1970) Burial diagenesis in Gulf Coast pelitic sediments: *Clays & Clay Minerals* **18,** 165–177.

Savage, D. and Chapman, N. A. (1982) Hydrothermal behavior of simulated waste-glass and waste-rock interactions under repository conditions: *Chem. Geology* **36,** 59–86.

Velde, B. (1973) Phase equilibria studies in the system MgO-$Al_2O_3$-$SiO_2$-$H_2O$: Chlorites and associated minerals: *Mineral. Mag.* **39,** 297–312.

Velde, B. and Hower, J. (1963) Petrological significance of

illite polymorphism in Paleozoic sedimentary rocks. *Amer. Mineral.* **48,** 1239–1254.

Yau, Y. C., Peacor, D. R., and McDowell, S. D. (1987) Smectite-to-illite reactions in Salton Sea shales: A transmission and analytical electron microscopy study: *J. Sed. Petrol.* **57,** 335–342.

Yoder, H. S. (1952) The $MgO$-$Al_2O_3$-$SiO_2$-$H_2O$ system and the related metamorphic facies: *Amer. J. Sci.* **Bowen Vol.,** 569–627.

*(Received 30 April 1986; accepted 9 February 1987; Ms. 1584)*